Organic–Inorganic Hybrid SiO$_2$ Supported Gold Nanoparticles: Facile Preparation and Catalytic Hydrogenation of Aromatic Nitro Compounds

Xiaoying Tan · Zhixin Zhang · Zihui Xiao ·
Qiang Xu · Changhai Liang · Xinkui Wang

Abstract Highly dispersed gold nanoparticles supported on organic–inorganic hybrid silica have been successfully prepared through a novel and facile approach. In the process, 3-aminopropyltriethoxysilane was hydrolyzed in HCHO aqueous solution to prepare silica with organic functional groups (–SiCH$_2$CH$_2$CH$_2$NHCH$_2$OH) formed through the reaction between –NH$_2$ and HCHO, then the silica reacted with HAuCl$_4$ in aqueous solution. Due to the reducibility of –SiCH$_2$CH$_2$CH$_2$NHCH$_2$OH, the gold precursor was in situ reduced on the silica. The materials were characterized by powder X-ray diffraction, transmission electron microscopy, Fourier-transform infrared spectroscopy, solid-state nuclear magnetic resonance spectroscopy, and X-ray photoelectron spectroscopy techniques. The results indicated Au nanoparticles were highly dispersed on silica with an average particles size 1.8 ± 0.5 nm. The as-obtained Au/SiO$_2$-org exhibited good catalytic activity and stability for liquid phase catalytic hydrogenation of aromatic nitro compounds with H$_2$.

Keywords In situ reduction · Organic–inorganic hybrid silica · Gold nanoparticles · Hydrogenation

1 Introduction

Following the discoveries by Haruta and Hutchings in the use of gold nanoparticles as catalysts for CO oxidation and ethyne hydrochlorination respectively in the 1980s, interest in catalysis by supported gold nanoparticles has dramatically expanded [1–5]. It is now generally accepted that the unexpected activity of supported gold catalysts is related to the particle size of gold, the nature of the support, and the preparation method [6–8]. At present, the main supports of gold catalysts are inorganic materials such as zeolite, amorphous SiO$_2$ or Al$_2$O$_3$ and activated carbon [9, 10]. However, due to the weak Van der Waals force between Au and carrier, leaching or aggregation of gold nanoparticles in high-temperature liquid reactions becomes one of the most important and challenging problems. In order to overcome the disadvantage of inorganic supports on which the active component is easy to leach into the solution, some complexes that can combine with the active component are introduced, forming organic–inorganic hybrid materials [11].

3-Aminopropyltriethoxysilane (APTES) is a common coupling agent that contains both hydrolysable –OC$_2$H$_5$ and non-hydrolysable organic hydrophobic groups –CH$_2$CH$_2$CH$_2$NH$_2$, which was widely used to prepare organic–inorganic NH$_2$–SiO$_2$ gel. Recently, a chemical grafting and reduction process was reported for preparation of this kind of gold catalysts, in which organosilanes with basic –NH$_2$ or –R$_4$N$^+$ moieties were introduced into the internal pore surfaces of pre-fabricated mesoporous silica. Gold ions were then introduced via a neutralization reaction between HAuCl$_4$ and the basic groups, followed by H$_2$ reduction to produce the supported gold nanocatalysts [12, 13]. Chen et al. [14] reported a novel synthetic method where the amino groups of APTES modified on SiO$_2$ can be used to anchor formaldehyde to form reductive species, which could in situ reduce AgNO$_3$ to form Ag nanoparticles. In addition, Sun et al. [15] utilized ^{13}C CP/MAS NMR spectroscopy to prove that the reductive species were –SiCH$_2$CH$_2$CH$_2$NHCH$_2$OH groups, and they fabricated monodispersed Ag nanoparticles in channels of mesoporous

X. Tan · Z. Zhang · Z. Xiao · Q. Xu · C. Liang · X. Wang (✉)
Laboratory of Advanced Materials and Catalytic Engineering,
School of Chemistry, Dalian University of Technology,
Dalian 116024, China
e-mail: xinkuiwang@sina.com

silica using a post chemical grafting method. However, for the above-mentioned methods, the preparation of silica and their surface modification with –NH$_2$ and then –NHCH$_2$OH are completely separated, requiring a long period of time, usually a few days, while the amount of –NHCH$_2$OH on silica is also limited for reducibility of metal ions.

Herein, we report a simple and convenient route to prepare supported gold nanoparticles on the surface of silica-based materials. During the process, HCHO not only plays the role of hydrolysis catalyst of APTES but also reacts with the amino of APTES to form an –NHCH$_2$OH group, which can reduce HAuCl$_4$. In this case, the –NHCH$_2$OH groups anchored on the silica network would act as linkage groups between inorganic material and the active component Au, and prevent Au nanoparticles from leaching when they are used in solutions. In comparison to similar Au catalysts prepared through the chemical grafting method in the literatures [11, 14, 15], more –NH$_2$ or –NHCH$_2$OH groups are on the silica surface and more gold ions would be reduced in situ because APTES has been adopted as the silicon source. Furthermore the organic groups around the Au nanoparticles may tune the electronic nature of Au, leading to favorable catalysis for some organic reactions. In fact, the present study of the catalytic hydrogenation of aromatic nitro compounds proves that the as-prepared Au-loaded catalysts exhibit enhanced activity and recycling stability.

2 Experimental

2.1 Catalyst Synthesis

The organic–inorganic hybrid silica supported gold nanoparticles were prepared as follows. First, 4.7 mL of APTES was added into 150 mL of deionized water. Then, 1.4 mL of HCHO (37 %) was added into the mixture under stirring, where immediately a white precipitate appeared. After stirring at room temperature for 2 h, the obtained solid was filtered and washed with an excess amount of deionized water. The solid was then dried in vacuum at 120 °C for 12 h, which yielded a solid white powder (denoted as SiO$_2$-org). Then 1.0 g of SiO$_2$-org was suspended in 30 mL of 1.62×10^{-3} mol L^{-1} HAuCl$_4$ aqueous solution. After stirring for 2 h at 100 °C, the mixture was filtered and washed with an excess amount of deionized water until no chlorine ions were detected in the filtrate. Following drying in vacuum at 120 °C for 12 h, a solid powder of Au/SiO$_2$-org material was obtained.

2.2 Characterizations

The actual gold loading of the catalysts was determined by inductively coupled plasma atomic emission spectroscopy

(ICP-AES). The materials were examined using transmission electron microscopy (TEM, Philips Tecnai G^2 20 equipped with a CCD camera operated at 200 kV). X-ray diffraction (XRD) patterns were recorded on a PW3040/60 X' Pert PRO (PANalytical) diffractometer (CuKa X-ray source, operated at 40 kV and 50 mA). The Fourier-transform infrared (FT-IR) spectra were acquired with a spectrometer (Bruker tensor27) equipped with a DLATGS detector and operated at a resolution of 4 cm^{-1}. X-ray photoelectron spectroscopy (XPS) spectra were obtained with a VG ESCALAB 250 equipped with a monochromated Al–Kα radiation source (1486.6 eV) under a residual pressure of 10^{-9} Torr. The binding energy scale was referenced to C1s at 284.6 eV. Solid-state ^{13}C CP/magic angle spinning nuclear magnetic resonance (MAS NMR) experiments were conducted in a Bruker Avance III 500 MHz NMR spectrometer equipped with a 4 mm standard bore probe head, using a magnetic field of 11.7 T at 296 K. The samples were packed in the ZrO$_2$ rotor closed with Kel-F cap, which were then spun at 5 kHz rate. A total of 512 scans were recorded with 5 s recycle delay for each sample. All ^{13}C MAS chemical shifts are referenced to the resonances of C$_2$H$_5$NO$_2$ standard ($\delta = -176.00$ ppm).

2.3 Catalytic Test

The catalytic hydrogenation of aromatic nitro compounds was performed in a 100 mL stainless steel autoclave with mechanical stirrer under the following reaction conditions: 140 °C, 4.0 MPa H$_2$, 0.1 g of catalyst, 0.5 g of substrates, and 40 mL of ethanol. The products were analyzed by a 7890F gas chromatograph equipped with a SE-54 capillary column and a flame ionization detector.

3 Results and Discussion

The Au/SiO$_2$-org catalyst was prepared via two major steps: (1) one-pot preparation of SiO$_2$-org with –SiCH$_2$CH$_2$CH$_2$NHCH$_2$OH groups; (2) in situ reduction of gold ions in aqueous solution to form gold nanoparticles on SiO$_2$-org. The method is easy to perform and no organic solvent such as toluene is used. This contrasts with the chemical grafting method, which has usually adopted a toluene solution of organic silane to anchor organic groups, and a much longer processing time. The ICP-AES analysis showed that the gold loading for Au/SiO$_2$-org was 0.99 %, essentially identical to the designed 1.0 %, proving a high efficiency of gold utilization. This is an advantage of this method considering that only a fraction of the gold ions used were deposited onto supports by using other reported preparation methods [16–18].
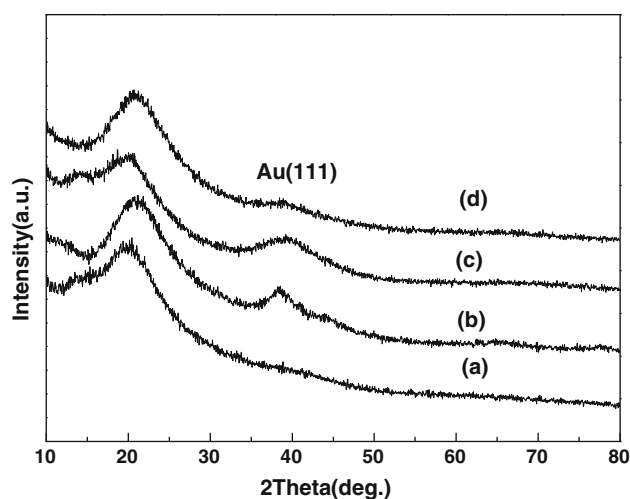
Fig. 1 XRD patterns of 1.0 % Au/SiO$_2$-org **a** fresh, **b** used and **c** 3.0 % Au/SiO$_2$-org, and **d** 1.0 % Au/SiO$_2$-org prepared by Chen method

Figure 1a shows the XRD pattern of fresh 1.0 % Au/SiO$_2$-org. No peaks due to Au were detected besides a diffraction peak of amorphous silica, implying that the gold particles are highly dispersed on the support. In order to clearly examine the metal particle size and size distribution of the gold catalysts, a high-resolution TEM technique was employed. From the TEM images of 1.0 % Au/SiO$_2$-org (Fig. 2a), the homogeneously dispersed gold nanoparticles with an average size 1.8 ± 0.5 nm were observed, which is well in agreement with the XRD result.

In order to clarify the surface state of Au nanoparticles, XPS was performed. For the fresh 1.0 % Au/SiO$_2$-org

(Fig. 3a), the binding energy of Au4f$_{7/2}$ is 83.4 eV, which is lower than that of bulk metallic gold (84.0 eV). Such a negative shift has also been observed with gold catalysts by other groups [19–21]. Arrii et al. [19] observed the dependence of the Au4f$_{7/2}$ binding energies on different kinds of supports, and concluded that the gold is in the metallic state, because they did not observe any peaks of oxidized gold species (located around 85.5 and 86.3 eV). They attributed such a negative shift to the possible electron transfer from the support to the particle. Hence, based on the above reports [19–21], we propose that Au in Au/SiO$_2$-org is of a metallic nature, and the 0.6 eV difference is due to the interaction between the organic groups on SiO$_2$-org and the Au nanoparticles, This in turn may provide the Au/SiO$_2$-org with high stability for catalysis.

Figure 4 shows the FT-IR spectra of SiO$_2$-org and 1.0 % Au/SiO$_2$-org between 4,000 and 400 cm^{-1}. The two spectra are similar in terms of peak profile other than peak intensities. Two bands at 2,935 and 2,872 cm^{-1} are observed, which conventionally are assigned to characteristic asymmetric and symmetric vibrations of the –CH$_2$ groups in the propyl chain of the APTES. In addition, the bands at 1,470 and 688 cm^{-1} are attributed to the scissor bending vibrations of the –CH$_2$–CH$_2$–CH$_2$– groups and the –CH$_2$ rocking vibration of Si–CH$_2$R, respectively [22, 23]. The band at 917 cm^{-1} is assigned to δ (N–H). The strong peaks are noted at 1,040 and 1,124 cm^{-1} due to the siloxane vibrations (Si–O–Si and Si–O–C) [11]. The band at 925 cm^{-1} is assigned to Si–OH stretching, while the two bands at 786 and 452 cm^{-1} are due to Si–O–Si [22]. The results of FT-IR characterization confirmed the existence
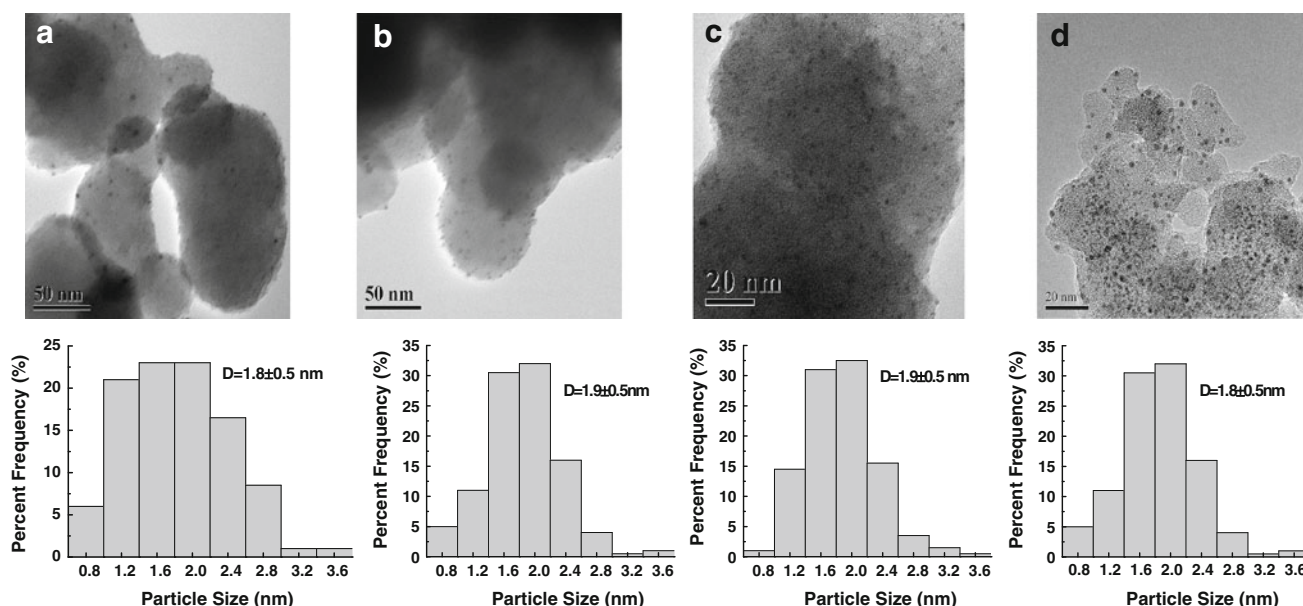

Fig. 2 TEM images and the corresponding particle size distributions of 1.0 % Au/SiO$_2$-org **a** fresh, **b** used, **c** 3.0 % Au/SiO$_2$-org, and **d** 1.0 % Au/SiO$_2$-org prepared by Chen method
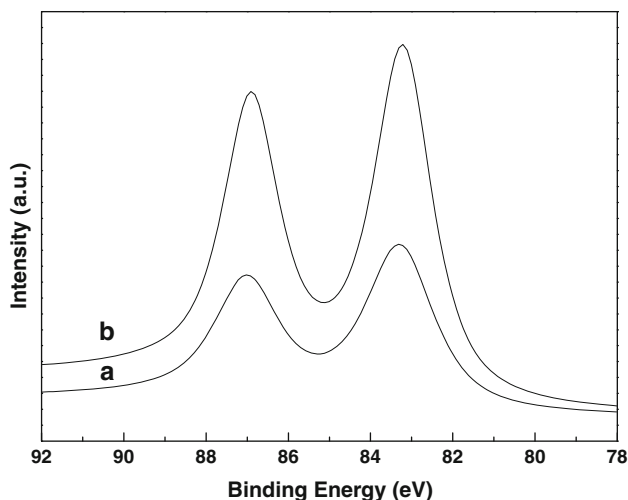
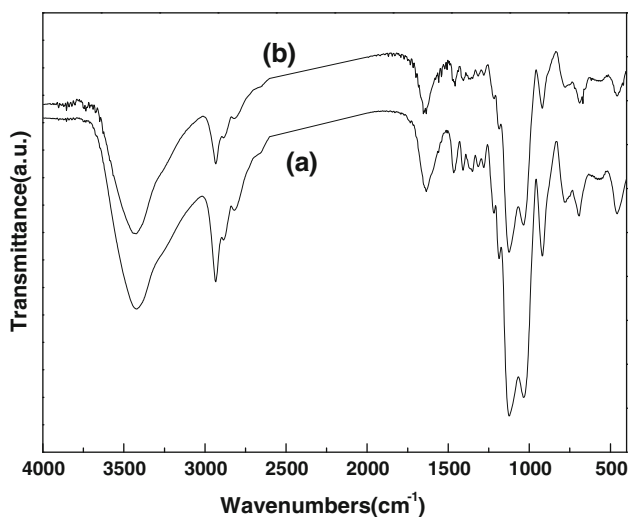**Fig. 3** XPS spectra of 1.0 % Au/SiO₂-org **a** fresh, **b** used

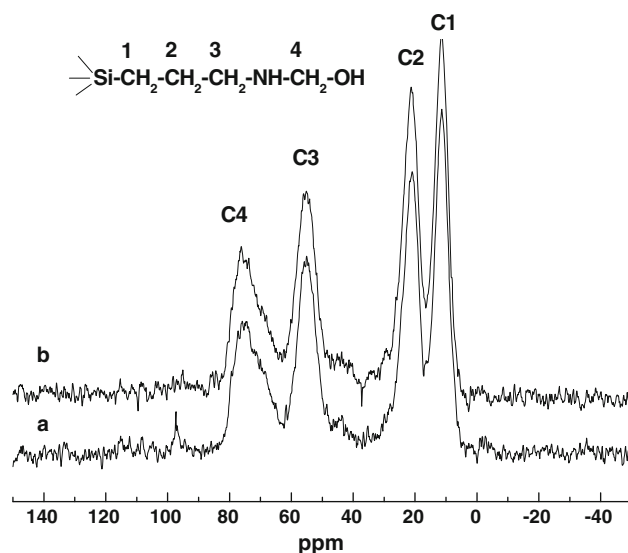**Fig. 4** FT-IR spectra of **a** 1.0 % Au/SiO₂-org, **b** SiO₂-org

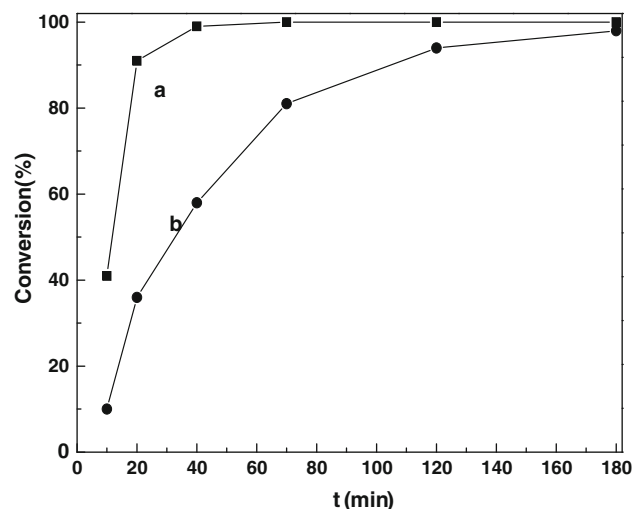**Fig. 5** ^{13}C CP/MAS NMR spectra of **a** SiO₂-org, **b** Au/SiO₂-org

Fig. 6 Reaction time dependence of *p*-CNB conversion over **a** our Au/SiO₂-org and **b** Au/SiO₂-org prepared by Chen method

of aminopropyl groups and the successful preparation of organic–inorganic hybrid silica [14, 15]. In addition, the results demonstrated that the reductive groups on the SiO₂-org can be observed even though 1.0 % Au was loaded on the support, and the gold nanoparticles had no influence on the FT-IR activities of organic groups surrounding them.

To investigate the formation mechanism of metal nanoparticles on the SiO₂-org support, ^{13}C CP/MAS NMR spectroscopy was employed. Figure 5a shows the ^{13}C CP/MAS NMR spectrum of as-synthesized SiO₂-org. The three strong signals at 12, 20, and 55 ppm can be ascribed to the resonances of the three methylene groups in the grafted aminopropyl moieties [24, 25]. The appearance of a peak at ca.76 ppm suggests that formaldehyde did react with the anchored amino groups, resulting in a new methylene group in –NHCH₂OH. However, compared with Sun's

report [15], the signal at 76 ppm doesn't disappear after the sample reacts with HAuCl₄ (Fig. 5b). We deduced that the quantity of -NHCH₂OH was too much relative to AuCl₄⁻ ions for the 1.0 % Au/SiO₂-org. Thus only a minority of -NHCH₂OH played a reductive role, which is in line with the FT-IR result. In order to prove this possibility, an Au/SiO₂-org with nominal 3.0 % gold loading has been prepared. The ICP-AES analysis confirms an actual Au loading of 2.9 %, and the XRD (Fig. 1c) and TEM (Fig. 2c) results show that the gold particles are still highly dispersed with an average particle size 1.9 ± 0.5 nm.
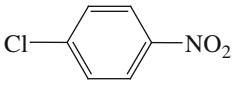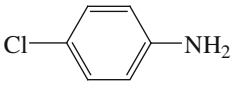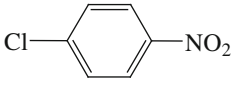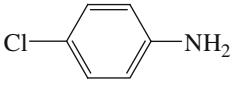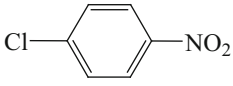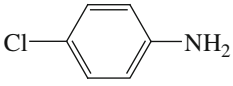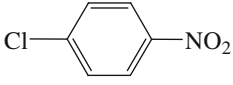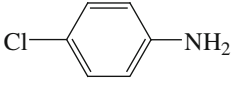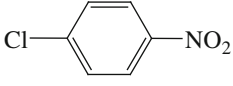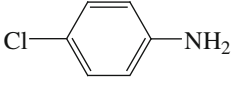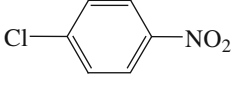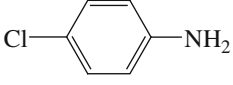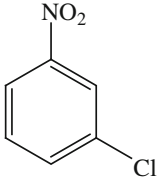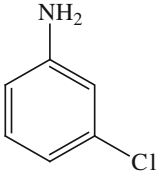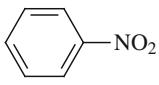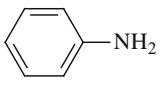
The hydrogenation of *p*-chloronitrobenzene (*p*-CNB) with H₂ was employed as a probe reaction to examine the catalytic performance of the as-synthesized Au/SiO₂-org.

For comparison, SiO$_2$-org supported Au catalyst was also prepared by the method of Chen et al. [14] by just changing Ag to Au. Our catalyst exhibited higher catalytic activity than that obtained by Chen et al. method (Fig. 6). For the catalyst by Chen et al. method, after 40 min of reaction at 140 °C and 4.0 MPa, the conversion was only 58 %, and it took 180 min to reach near 100 %; however, in our case the conversion reached 99 % after 40 min and 100 % after 70 min. In order to investigate the influence of reaction temperature on the conve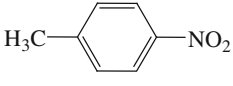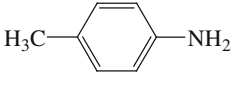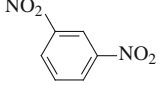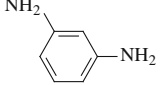rsion and the selectivity, the hydrogenation of p-CNB was performed at 100 °C. The conversion of p-CNB was only 33 % for 40 min, the selectivity of p-chloroaniline was 67 %, and the byproduct was chlorine-containing nitroso compound, a kind of reaction intermediate for the hydrogenation of nitro aromatic compounds. Further increasing the reaction time to 120 min, the conversion increased significantly to reach 99 %, and the selectivity of p-chloroaniline was improved to 80 %, proving that chlorine-containing nitroso compound could be further hydrogenated to p-chloroaniline.

To uncover the underlying reason for the difference of catalytic activity, we examined the gold particle size distribution on the two catalysts by means of XRD and TEM. From the TEM images (Fig. 2a, d), it can be seen that the

Table 1 Catalytic hydrogenation of various aromatic nitro compounds over Au/SiO$_2$-org

Entry	Substrate	Product	T (°C)	Time (min)	Conv. (%)	Sel. (%)
1	Cl—⟨ ⟩—NO$_2$	Cl—⟨ ⟩—NH$_2$	100	40	33	67[a]
2	Cl—⟨ ⟩—NO$_2$	Cl—⟨ ⟩—NH$_2$	100	120	>99	80[a]
3	Cl—⟨ ⟩—NO$_2$	Cl—⟨ ⟩—NH$_2$	140	40	99	99
4[b]	Cl—⟨ ⟩—NO$_2$	Cl—⟨ ⟩—NH$_2$	140	40	99	98
5[c]	Cl—⟨ ⟩—NO$_2$	Cl—⟨ ⟩—NH$_2$	140	40	95	90
6	Cl—⟨ ⟩—NO$_2$	Cl—⟨ ⟩—NH$_2$	140	120	>99	96
7	NO$_2$ / Cl (meta)	NH$_2$ / Cl (meta)	140	120	>99	98
8	⟨ ⟩—NO$_2$	⟨ ⟩—NH$_2$	140	120	>99	100
9	H$_3$C—⟨ ⟩—NO$_2$	H$_3$C—⟨ ⟩—NH$_2$	140	120	>99	97
10	NO$_2$ / NO$_2$ (meta)	NH$_2$ / NH$_2$ (meta)	140	360	>99	95

Reaction conditions: 4.0 MPa H$_2$, 0.1 g of catalyst, 0.5 g of substrates, and 40 mL of ethanol

[a] The byproduct was hydrogenation intermediate (chlorine-containing nitroso compound)

[b] Catalyst was filtered off after the 1st reaction cycle (entry 3) and the substrate was added for the second reaction cycle

[c] Catalyst after the 2nd reaction cycle (entry 4) was adopted

sizes of gold particles are 1.8 ± 0.5 nm, which are well in agreement with the XRD results (Fig 1a, d), implying that the dispersions of our catalyst and the catalyst by Chen et al. method are almost the same. So the enhanced activity of our sample could be attributed to the more organic groups around the Au nanoparticles, which may tune the electronic nature of Au, leading to favorable catalysis for organic reactions. When HAuCl$_4$ and SiO$_2$-org were separately used as catalysts for the reaction, no reduction products were detected. This confirms that it is the gold nanoparticles on Au/SiO$_2$-org that function as real active sites. The catalytic reductions of various aromatic nitro compounds over Au/SiO$_2$-org were also examined. From Table 1, it can be concluded that the conversion of several substrates and selectivity of products could reach nearly 100 % and >95 %, respectively. However, the formation of nitroso compound intermediate cannot be totally avoided.

To test the stability of Au/SiO$_2$-org, the catalyst was used repeatedly for consecutive hydrogenation of *p*-CNB (Table 1), which shows that no significant loss in catalytic efficiency for 40 min was found after three cycles at 140 °C and 4.0 MPa. The ICP-AES of gold loading for the used Au/SiO$_2$ catalyst was 0.98 %, approximate to 0.99 % of the fresh catalyst, proving no significant gold leaching during the reaction process. For the XRD pattern of the used Au/SiO$_2$-org (Fig. 1b), a very weak and broad peak at $2\theta = 38.2°$ due to very small crystalline gold particles can be observed (PDF 04-0783), indicating that during the recycle process the size of gold particles slightly changed. The TEM characterization of the used sample (Fig. 2b) showed that there was no aggregation of gold nanoparticles after catalytic application in the high-temperature liquid reactions, which was attributed to the interaction of organic groups and Au nanoparticles. In addition, the XPS spectrum of used 1.0 %Au/SiO$_2$-org (Fig. 3b) has a negative shift of 0.1 eV in comparison with the fresh catalyst, which indicates the adsorption of organic species during the hydrogenation reaction.

4 Conclusions

APTES as a silicon source was hydrolyzed in HCHO aqueous solution to prepare silica with organic functional groups (–SiCH$_2$CH$_2$CH$_2$NHCH$_2$OH). Because of the reducibility of –SiCH$_2$CH$_2$CH$_2$NHCH$_2$OH, the HAuCl$_4$ in aqueous solution were in situ reduced on the organic–inorganic hybrid silica. The highly dispersed and uniform gold nanoparticles on the silica show high activity and selectivity for hydrogenation of aromatic nitro compounds to the corresponding aromatic amino compounds. The Au/SiO$_2$-org without any pre-treatment shows good stability, with little change in the particle size of the gold nanoparticles in the used compared to the fresh catalyst. The enhanced catalytic efficiency was mainly due to the more organic groups around the Au nanoparticles. This new route provides a useful platform for the fabrication of metal nanoparticles (such as Pd and Pt) based on SiO$_2$ grafted with –NH$_2$ by altering the metal precursors. This methodology should therefore prove to be useful in catalysis and other fields.

References

1. Hutchings GJ (1985) J Catal 96:292
2. Haruta M, Kobayashi T, Sano H, Yamada N (1987) Chem Lett 16:405
3. Haruta M, Yamada N, Kobayashi T, Iijima S (1989) J Catal 115:301
4. Hughes MD, Xu YJ, Jenkins P, McMorn P, Landon P, Enache DI, Carley AF, Attard GA, Hutchings GJ, King F, Stitt EH, Johnston P, Griffin K, Kiely CJ (2005) Nature 437:1132
5. Enache DI, Edwards JK, Landon P, Solsona-Espriu B, Carley AF, Herzing AA, Watanabe M, Kiely CJ, Knight DW, Hutchings GJ (2006) Science 311:362
6. Boccuzzi F, Chiorino A, Manzoli M, Lu P, Akita T, Ichikawa S, Haruta M (2001) J Catal 202:256
7. Wolf A, Schüth F (2002) Appl Catal A 226:1
8. Schubert MM, Hackenberg S, Veen ACV, Muhler M, Plzak V, Behm RJ (2001) J Catal 197:113
9. Li G, Enache DI, Edwards J, Carley AF, Knight DW, Hutchings GJ (2006) Catal Lett 110:7
10. Haruta M, Tsubota S, Kobayashi T, Kageyama H, Genet MJ, Delmon B (1993) J Catal 144:175
11. Chen YY, Qiu JS, Wang XK, Xiu JH (2006) J Catal 242:227
12. Gu JL, Shi JL, You GJ, Xiong LM, Qian SX, Hua ZL, Chen HR (2005) Adv Mater 17:557
13. Yang CM, Sheu HS, Chao KJ (2002) Adv Funct Mater 12:143
14. Chen YY, Wang C, Liu H, Qiu JS, Bao XH (2005) Chem Commun 42:5298
15. Sun JM, Ma D, Zhang H, Liu XM, Han XW, Bao XH, Weinberg G, Pfänder N, Su DS (2006) J Am Chem Soc 128:15756
16. Liu YX, Xing TF, Luo YM, Li XN, Yan W (2010) Chin Chem Lett 21:1322
17. Ma CY, Cheng J, Wang HL, Hu Q, Tian H, He C, Hao ZP (2010) Catal Today 158:246
18. Zahmalran M, Özkar S (2010) Mater Chem Phys 121:359
19. Arrii S, Morfin F, Renouprez AJ, Rousset JL (2004) J Am Chem Soc 126:1199
20. Radnik J, Mohr C, Claus P (2003) Phys Chem Chem Phys 5:172
21. Zwijnenburg A, Goossens A, Sloof WG, Craje' MWJ, Van der Kraan AM, Jos de Jongh L, Makkee M, Moulijn JA (2002) J Phys Chem B 106:9853–9862
22. Lou LL, Jiang S, Yu K, Gu ZC, Ji RN, Dong YL, Liu SX (2011) Micro Mes Mater 142:214
23. Wang HL, Zhao R, Yan L, Ding Y, Suo JS (2006) J Mol Catal 20:1
24. Liu AM, Hidajat K, Kawi S, Zhao DY (2000) Chem Commun 13:1145
25. Huh S, Wiench JW, Yoo JC, Pruski M, Lin VSY (2003) Chem Mater 15:4247